Theses and Dissertations | 1. Thesis and Dissertation Collection, all items

1991-12

Acoustically probed Taylor-Couette flow apparatus

Blum, Kevin M.

Monterey, California. Naval Postgraduate School

http://hdl.handle.net/10945/27925

NAVAL POSTGRADUATE SCHOOL
Monterey, California

THESIS

ACOUSTICALLY PROBED TAYLOR-COUETTE
FLOW APPARATUS

by

Kevin M. Blum

December, 1991

| Co-Advisor | Anthony Atchley |
| Co-Advisor | Andrés Larraza |

Approved for public release; distribution is unlimited.

REPORT DOCUMENTATION PAGE

1a REPORT SECURITY CLASSIFICATION Unclassified		1b RESTRICTIVE MARKINGS			
2a SECURITY CLASSIFICATION AUTHORITY		3 DISTRIBUTION/AVAILABILITY OF REPORT Approved for public release; distribution is unlimited.			
2b DECLASSIFICATION/DOWNGRADING SCHEDULE					
4 PERFORMING ORGANIZATION REPORT NUMBER(S)		5 MONITORING ORGANIZATION REPORT NUMBER(S)			
6a NAME OF PERFORMING ORGANIZATION Naval Postgraduate School	6b OFFICE SYMBOL (If applicable) 33	7a NAME OF MONITORING ORGANIZATION Naval Postgraduate School			
6c. ADDRESS (City, State, and ZIP Code) Monterey, CA 93943-5000		7b ADDRESS (City, State, and ZIP Code) Monterey, CA 93943-5000			
8a NAME OF FUNDING/SPONSORING ORGANIZATION	8b OFFICE SYMBOL (If applicable)	9 PROCUREMENT INSTRUMENT IDENTIFICATION NUMBER			
8c. ADDRESS (City, State, and ZIP Code)		10 SOURCE OF FUNDING NUMBERS			
		PROGRAM ELEMENT NO	PROJECT NO	TASK NO	WORK UNIT ACCESSION NO

11 TITLE (Include Security Classification)

ACOUSTICALLY PROBED TAYLOR-COUETTE FLOW APPARATUS

12 PERSONAL AUTHOR(S)
Kevin M. Blum

13a TYPE OF REPORT Master's Thesis	13b TIME COVERED FROM _____ TO _____	14 DATE OF REPORT (Year, Month, Day) December 1991	15 PAGE COUNT 38

16 SUPPLEMENTARY NOTATION
The views expressed in this thesis are those of the author and do not reflect the official policy or position of the Department of Defence or the U.S. Government.

17	COSATI CODES		18 SUBJECT TERMS (Continue on reverse if necessary and identify by block number)
FIELD	GROUP	SUB-GROUP	Taylor-Couette Flow, Acoustic Phase, Turbulence

19 ABSTRACT (Continue on reverse if necessary and identify by block number)

   A Taylor-Couette cell for the investigation of geometrical phase in acoustics has been constructed. The inner and outer cylinders are made of acrylic. The cell has an inner cylinder radius of 9.477 cm, radius ratio of 0.902, and cavity aspect ratio of 49.2. Two high performance d.c. motors can rotate the cylinders independently. The angular speed of the cylinders is monitored by a photo-interrupter. A piezoelectric polymer (PVDF) transducer mounted on the inner cylinder drives the acoustic field in the cavity and a 6.02 mm diameter electret microphone embedded in the wall of the inner cylinder acts a receiver. Static measurements of the acoustic modes in the annular cavity show good agreement with theory, though measurements at different angular locations of the transducer reveal 2% non-uniformities. The effects of non-uniformities could be overcome by rotating the cylinders at high speeds. The performance under these preliminary tests indicate that an apparatus of this design is suitable for investigations of acoustics in rotating flows.

20. DISTRIBUTION/AVAILABILITY OF ABSTRACT ☐ UNCLASSIFIED/UNLIMITED ☐ SAME AS RPT ☐ DTIC USERS	21 ABSTRACT SECURITY CLASSIFICATION Unclassified	
22a NAME OF RESPONSIBLE INDIVIDUAL A. Atchley	22b TELEPHONE (Include Area Code) (408)646-2848	22c OFFICE SYMBOL Ph-ay

Acoustically Probed Taylor-Couette
Flow Apparatus

by

Kevin M. Blum
Lieutenant, United States Navy
B.S., United States Naval Academy, 1984

Submitted in partial fulfillment
of the requirements for the degree of

MASTER OF SCIENCE IN ENGINEERING ACOUSTICS

from the

NAVAL POSTGRADUATE SCHOOL
December 1991

Anthony A. Atchley, Chairman
Engineering Acoustics Academic Committee

ii

ABSTRACT

A Taylor-Couette cell for the investigation of geometrical phase in acoustics has been constructed. The inner and outer cylinders are made of acrylic. The cell has an inner cylinder radius of 9.477 cm, radius ratio of 0.902, and cavity aspect ratio of 49.2. Two high performance d. c. motors can rotate the cylinders independently. The angular speed of the cylinders is monitored by a photo-interrupter. A piezoelectric polymer (PVDF) transducer mounted on the inner cylinder drives the acoustic field in the cavity and a 6.02 mm diameter electret microphone embedded in the wall of the inner cylinder acts as a receiver. Static measurements of the acoustic modes in the annular cavity show good agreement with theory, though measurements at different angular locations of the transducer reveal 2% nonuniformities. The effects of nonuniformities could be overcome by rotating the cylinders at high speeds. The performance under these preliminary tests indicate that an apparatus of this design is suitable for investigations of acoustics in rotating flows.

TABLE OF CONTENTS

I. INTRODUCTION

The motion of a fluid flow between two concentric, long cylinders undergoing differential rotation has been one of the most studied problems in hydrodynamics (Donnelly, 1991), with however, numerous unanswered questions. Such fluid motion is called Taylor-Couette flow.

The steady state axis-symmetric flow is an exact solution of the Navier-Stokes equation in this configuration. This flow is simply described as the superposition of solid body rotation plus the flow of a vortex line along the common axis of the two cylinders. When the inner cylinder is turned at a higher rate, such that the inner layers of the fluid are moving more rapidly than the outer ones, the centrifugal force pulls these inner layers outward which then break into cells and circulate. The fluid breaks into horizontal bands. Thus, the axis-symmetric flow is, in general, not stable. As the angular velocity of the inner cylinder is increased, the number of bands increases at first, then they become wavey. The velocity of rotation of this wavey pattern approaches a numerical constant (which is determined by the geometrical parameters of the system) times the angular velocity of the cylinder. Finally, for higher values of the angular velocity, or in the configuration in which the outer cylinder is rotating in the opposite direction, the flow becomes turbulent.

The complexity of behavior in this simple system is in principle contained in the equations of a viscous fluid. However, there does not exist, up to the present, a satisfactory method to analyze and explain the complexities hidden in the Navier-Stokes equation: instabilities, the onset of turbulent flows, and intermittency.

Consider however, the flow not as a dynamical system, but as a collection of parameters of an acoustic field. In the geometrical acoustic approximation, the acoustic field is described by an equation analogous to Schrödinger's equation of a charged particle, with the flow velocity playing the role of the magnetic vector potential. Then, it is possible to determine global properties of the flow by measurements of the acoustic phase. Modal resonance splitting and shifting are manifestations of global changes.

This thesis describes the design, construction, and preliminary testing of a Taylor-Couette cell. The flow apparatus is designed with maximum flexibility in mind. Preliminary testing and experimentation using the cell determined its suitability for future research.

The organization of this thesis is as follows. Chapter II presents the theory for the mode structure of the Taylor-Couette cell in its static and differential rotation configurations. Chapter III describes the design and construction of the cell. Chapter IV describes the

preliminary tests and their results. Chapter V presents a summary and conclusions of this work.

II. THEORY

A. EXPECTED RESONANCE FREQUENCIES

In order to observe the modal frequency split and shift in a rotating circular Couette system, we require knowledge of the modal structure. The following theory derives those frequencies.

Consider the annular cavity formed by two concentric cylinders of inner and outer radii, R_i and R_o, respectively, with top and bottom boundaries located at $z=0$ and $z=L_z$. If all surfaces of the cavity are perfectly rigid, so that the particle velocity normal to the surface is zero, then for linear acoustics $\hat{n} \cdot \nabla p = 0$ at all boundaries, where ∇p is the gradient of the acoustic pressure. Thus

$$\left(\frac{\partial p}{\partial r}\right)_{r=R_i} = \left(\frac{\partial p}{\partial r}\right)_{r=R_o} = 0,$$

$$\left(\frac{\partial p}{\partial z}\right)_{z=0} = \left(\frac{\partial p}{\partial z}\right)_{z=L_z} = 0. \tag{1}$$

For a system with circular symmetry, it is best to recast the linear inviscid wave equation in polar coordinates

$$\frac{\partial^2 p}{\partial r^2} + \frac{1}{r}\frac{\partial p}{\partial r} + \frac{1}{r^2}\frac{\partial^2 p}{\partial \theta^2} + \frac{\partial^2 p}{\partial z^2} = \frac{1}{c^2}\frac{\partial^2 p}{\partial t^2}, \tag{2}$$

4

where c is the speed of sound of the medium. The technique of separation of variables is use to solve Eq. (2). The acoustic pressure is assumed to be a product of four terms, each a function of only one variable, i.e.

$$p(r,\theta,z,t) = R(r)\Theta(\theta)Z(z)e^{j\omega t}. \tag{3}$$

Substitution of Eq. (3) into Eq. (2) yields

$$\Theta Z\frac{d^2R}{dr^2} + \frac{\Theta Z dR}{rdr} + \frac{RZ d^2\Theta}{r^2 d\theta^2} + \frac{R\Theta d^2Z}{dz^2} + k^2R\Theta Z = 0, \tag{4}$$

where k=ω/c. Multiplying each term in this equation by 1/RΘZ and grouping terms containing z on one side results in

$$\frac{d^2R}{Rdr^2} + \frac{1dR}{rRdr} + \frac{1d^2\Theta}{r^2\Theta d\theta^2} + k^2 = \frac{-1d^2Z}{Zdz^2}. \tag{5}$$

The left-hand side of this equation, a function of r and θ, cannot be equal to the right-hand side, a function of z alone, unless both functions equal some constant. If we let this constant be k_z^2, the right-hand side becomes

$$\left(\frac{d^2}{dz^2} + k_z^2\right)Z = 0. \tag{6}$$

Repeated performance of the separation of variables technique applied to Eq. (4) results in the final set of equations:

$$\left[\frac{d^2}{dz^2} + k_z^2\right]Z = 0, \tag{7a}$$

$$\left[\frac{d^2}{d\theta^2} + m^2\right]\Theta = 0, \tag{7b}$$

$$\left[\frac{d^2}{dr^2} + \frac{1}{r}\frac{d}{dr} + \left(k_m^2 - \frac{m^2}{r^2}\right)\right]R = 0, \tag{7c}$$

where m^2 is an arbitrary separation constant and $k_m{}^2 = k^2 - k_z{}^2$.

The complete general solution to Eq. (7a) is

$$Z(z) = A_1\cos(k_z z) + A_2\sin(k_z z), \tag{8}$$

where A_1 and A_2 are arbitrary constants. The solution to Eq. (7b) is

$$\Theta(\theta) = B\cos(m\theta + \phi), \tag{9}$$

where B is an arbitrary constant and ϕ is an arbitrary phase angle dependent on the location of the source. Eq. (7c) is known as Bessel's equation. Solutions to this equation are the transcendental functions called Bessel functions of the first kind $J_m(k_m r)$ and second kind $Y_m(k_m r)$ of order m,

$$R(r) = C_1 J_m(k_m r) + C_2 Y_m(k_m r), \tag{10}$$

where C_1 and C_2 are arbitrary constants. Bessel functions are oscillating functions whose amplitudes decrease as their

6

arguments increase. The second kind functions $Y_m(k_m r)$, also known as Neumann functions, become unbound in the limit as $k_m r$ approaches zero.

Applying the appropriate boundary conditions to Eq. (8) results in

$$Z(z) = A_1 \cos(k_z z),$$

where

$$k_z = \frac{\ell \pi}{L_z} \qquad \ell = 0,1,2,\ldots \quad . \tag{11}$$

If the acoustic pressure p is to be a single-valued function of position, then $p(r,\theta,z,t)$ must equal $p(r,\theta+2\pi,z,t)$, which restricts the separation constant m to integral values; $m = 0, \pm 1, \pm 2, \ldots$.

When $k_m = 0$ and $m = 0$, Eq. (10) implies the solution

$$R(r) = C_1 = constant. \tag{12}$$

When k_m is non-zero, the boundary conditions applied to Eq. (10) results in the equality

$$\frac{J_m'(k_m R_1)}{Y_m'(k_m R_1)} = \frac{J_m'(k_m R_0)}{Y_m'(k_m R_0)}, \tag{13}$$

where the prime denotes the first derivative with respect to kr evaluated at the specified argument. If we let the ratio $R_0/R_1 = g$, then Eq. (13) can be written as

7

$$\frac{J'_m(k_m R_\iota)}{Y'_m(k_m R_\iota)} - \frac{J'_m(g k_m R_\iota)}{Y'_m(g k_m R_\iota)} = 0. \tag{14}$$

The roots of Eq. (14), values of $k_m R_\iota$, can be solved for using a computer for various values of m (see Appendix). If the values of the m_{th} order Bessel functions which cause Eq. (14) to equal zero are designated by j_{mn}, then the allowed values of k_m assume discrete values given by $k_{mn} = j_{mn}/R_\iota$.

Appropriate solutions to Eq. (3) for the case k_{mn} not equal to zero yield the normal modes

$$p_{\ell mn}(r,\theta,z,t) = P_{\ell mn}\left[Y_m(k_{mn}r) - \frac{Y'_m(k_{mn}R_\iota)}{J'_m(k_{mn}R_\iota)} J_m(k_{mn}r) \right] \tag{15}$$

$$\times \cos(m\theta + \phi) \cos(k_z z) \; e^{j\omega_{\ell mn}t},$$

where

$$k^2 = \frac{\omega^2}{c^2} = k_{mn}^2 + k_z^2$$

$$k_z = \frac{\ell\pi}{L_z} \qquad \ell = 0,1,2\ldots$$

$$k_{mn} = \frac{j_{mn}}{R_\iota} \qquad m = 0,1,2\ldots$$

$$n = 0,1,2\ldots$$

$$m = n \neq 0 . \tag{16}$$

The allowed frequencies are thus quantized by the relationship

$$f_{\ell mn} = \frac{c}{2\pi} \sqrt{k_{mn}^2 + k_z^2} \ . \tag{17}$$

Each eigenfunction given by Eq. (15) has its own characteristic eigenfrequency, denoted by Eq. (17), and can be specified by the ordered integers (ℓ, m, n). The value of ℓ determines the number of nodal surfaces in pressure perpendicular to the z axis. The value of m specifies the number of radial pressure nodes. The value of n gives the number of nodal surfaces of constant r (cylinders) surrounding the z axis and concentric with it.

Solutions to Eq. (3) when k_{mn} equals zero yield the normal modes

$$p_{\ell,0,0} \ (r, \theta, z, t) = P_{\ell,0,0} \cos(k_z z) \, e^{j\omega t},$$

where

$$k^2 = \frac{\omega^2}{c^2} = k_z^2$$

$$k_z = \frac{\ell\pi}{L_z} \quad \ell = 0, 1, 2, \ldots \quad . \tag{18}$$

The allowed frequencies are

$$f_{\ell,0,0} = \frac{c}{2\pi} k_z \ , \tag{19}$$

corresponding to pure z modes.

B. MODE STRUCTURE FOR DIFFERENTIAL ROTATION

Axis-symmetric flows in a Taylor-Couette cell are derived for the annular cavity between two infinitely long cylinders. However, the expected resonance frequencies derived assumed finite length cylinders. A justification for assuming such velocity field has been given previously by Andereck et al., 1983. These researchers noted that if the aspect ratio Γ, the ratio of the fluid height to the gap between the cylinders, at the region of measurement is properly chosen, then the boundary conditions existing at the top and bottom of the cylinders exerted no observable difference in the flow state properties. In other words, boundary conditions at the top and bottom of the cylinders can be neglected if measurements are made far removed from these boundaries. Many of the measurements cited in the above study were conducted with an aspect ratio of 30. However, other measurements were made with $20 \leq \Gamma \leq 47$. Our initial testing is conducted with $\Gamma = 24.6$. Therefore, we can assume that our region of interest has an azimuthally symmetric velocity field.

Consider waves with high azimuthal numbers m. For these waves the velocity field induced by the cylinders' differential rotation varies over distances large compared with the wavelength. Within this approximation, the local dispersion relation in the moving medium with velocity flow

$\vec{u}(\vec{r})$ is given by

$$\omega = \overline{\omega}(\vec{k}) + \vec{k} \cdot u(\vec{r}), \tag{20}$$

where $\overline{\omega}(\vec{k})$ is the dispersion relation of a wave with wave

vector $\vec{k}$ in the stationary medium. A particular realization

of the flow velocity is given by the stable azimuthal
configuration with a stationary inner cylinder. For flow
velocities $|u| \ll c$, Eq. (20) can be written to lowest order as

$$\omega = \overline{\omega}(|\vec{k} + \frac{k\vec{u}}{c}|, \vec{r}). \tag{21}$$

The correspondence between ω and the Hamiltonian establishes
the analogy between the magnetic vector potential A and the
flow velocity, provided

$$\frac{q}{h} \vec{A} \leftrightarrow \frac{-k\vec{u}}{c}. \tag{22}$$

(Berry et al., 1980; Larraza, 1989) Making the natural

identification between the wave vector $\vec{k}$ and the operator

$-i\nabla$, Eq. (21) is analogous to Schrödinger's equation for a

charged particle in a vector potential $\vec{A}$. The geometry of

Taylor-Couette flow for the azimuthally symmetric case yields
the eigenfrequency spectrum

$$\frac{\omega}{c} \approx \frac{1}{R_o}\left|m + \frac{|m|\Omega R_o}{c}\right| \tag{23}$$

(Larraza, 1989), valid for rotation of the outer cylinder only. If the rotational speed $\Omega=0$, the states $m\neq0$ are doubly degenerate. For a non-zero value of the rotational speed the degeneracy is broken. Physically, this means that the waves travelling in the same direction as the average flow have an additional contribution to the sound speed, whereas waves travelling in opposite direction to the flow have an effective sound speed which is less than the static value. According to Eq. (23), there is an asymmetric splitting of the degenerate states about the zero-angular speed eigenfrequency. To see this, notice that Eq. (23) is the first order expansion of

$$\frac{\omega}{c} = \left|\frac{\frac{m}{R_o}}{1\pm\frac{\Omega R_o}{c}}\right| . \tag{24}$$

For $\frac{|m|\Omega R_o}{c}=\frac{n}{2}$ with n an integer, degeneracy occurs. For n=1, the states m=1 and m=-2 are degenerate with frequency $\omega = \frac{3c}{2R_o}$, while the state m=-1 is not degenerate. Physically, these states are reached by increasing the rotational speed Ω and correspond to high azimuthal numbers m.

12

III.   TAYLOR-COUETTE FLOW APPARATUS

A.   MECHANICAL DESIGN

With flexibility in mind, the cell is designed to allow the inner and outer cylinders to be rotated independently. Also, rigid boundaries at the top and bottom of the cylinders allow for three types of boundary motion: stationary, rotation at the angular speed of the inner cylinder, and rotation at the angular speed of the outer cylinder.   The system is designed to be vertically mounted to eliminate flexural strain resulting from the weight of the components if mounted in a horizontal configuration.

1. Cylinders

The inner and outer cylinders are made of acrylic. The acrylic is fabricated using extruded, vice cast, methods, which introduced nonuniformity effects which will be described later.   The inner cylinder radius, R_i, is 9.477 cm and the outer cylinder radius, R_o, is 10.510 cm. The resulting radius ratio is 0.902, which is near the value used in many previous studies of Taylor-Couette flow. (DiPrima and Swinney, 1981) The solid boundaries used to enclose the annulus create a resonant cavity height, L_z, of 50.838 cm, resulting in a cavity aspect ratio of 49.2.

13

2. Support Structure and Bearings

With the exception of the cylinders, drive motors and their associated drive belts, the entire assembly, including support structures, are made of aluminum. The inner cylinder is supported by a length of solid round stock, with a diameter of 5.08 cm, which also provides axial alignment for the bearings.

Radial bearings are used to support rotating components since radial rigidity is of paramount importance. The type of radial bearings chosen are able to handle compound loads. Thus, while providing rigidity, they are also able to support load resulting from the weight of the assembly.

3. Upper and Lower Boundaries

Aluminum rings provide an acoustically rigid boundary condition. The rings can either be stationary, or rotated with the same angular speed as the cylinder to which they are attached. The rings are machined to fit flush against the cylinder they are connected to while providing as narrow a gap as possible near the other cylinder. While a tight cavity is desirable to set up standing waves, some gap between the rings and the cylinder walls is necessary to eliminate frictional rubbing which results in torque disturbance and noise pick-up on the receiver. The average gap between ring and cylinder wall is 0.01 in.

4. Motors and Drive Belts

Two high performance, fractional horsepower, disc-armature, dc motors are used to rotate the cylinders. These motors, PMI U-series model #U12M4H, are designed for excellent speed control and constant torque delivery. The motors are connected to the geared cylinders via a stainless steel cable reinforced, polyurethane, toothed drive belt.

5. Miscellaneous

The entire assembly is mounted on a 2 cm thick aluminum baseplate measuring 50 cm by 62 cm. Two vertical aluminum cylinders support a horizontal crossbar which provides axial alignment of the components at the top of the assembly. Figures 1, 2, and 3 show the construction of the apparatus as well as close-ups of the drive assembly and top cylinder mounting.
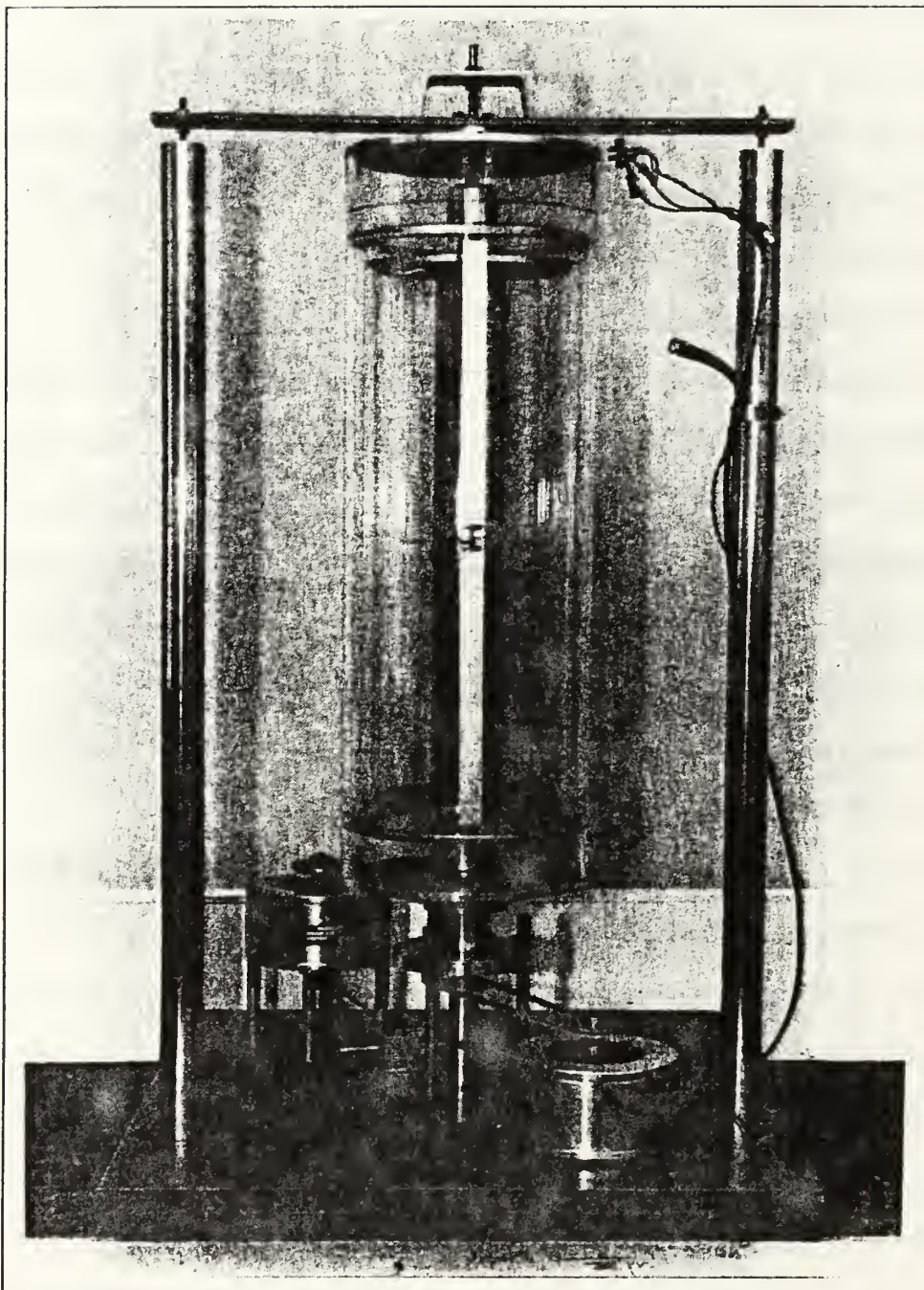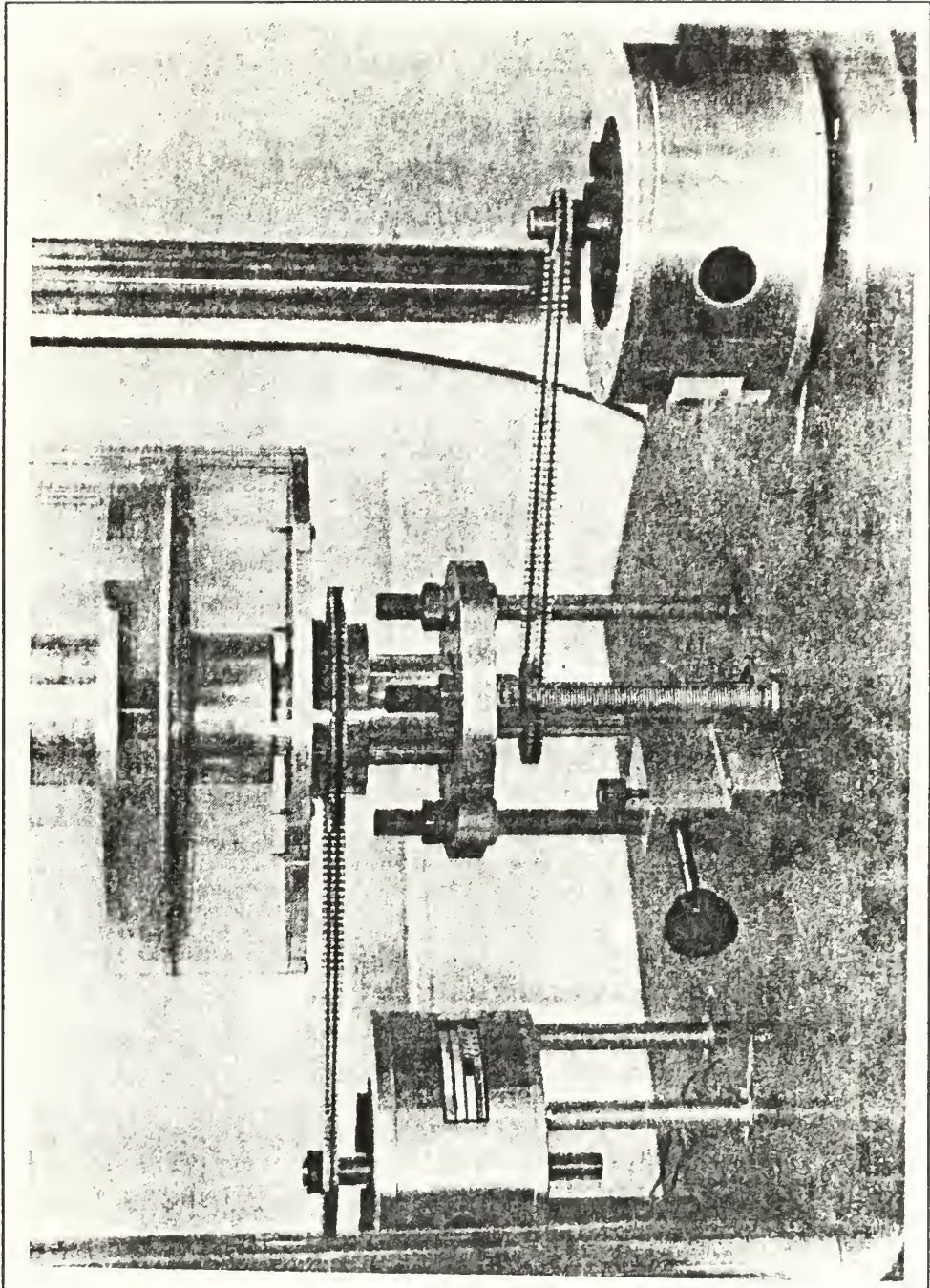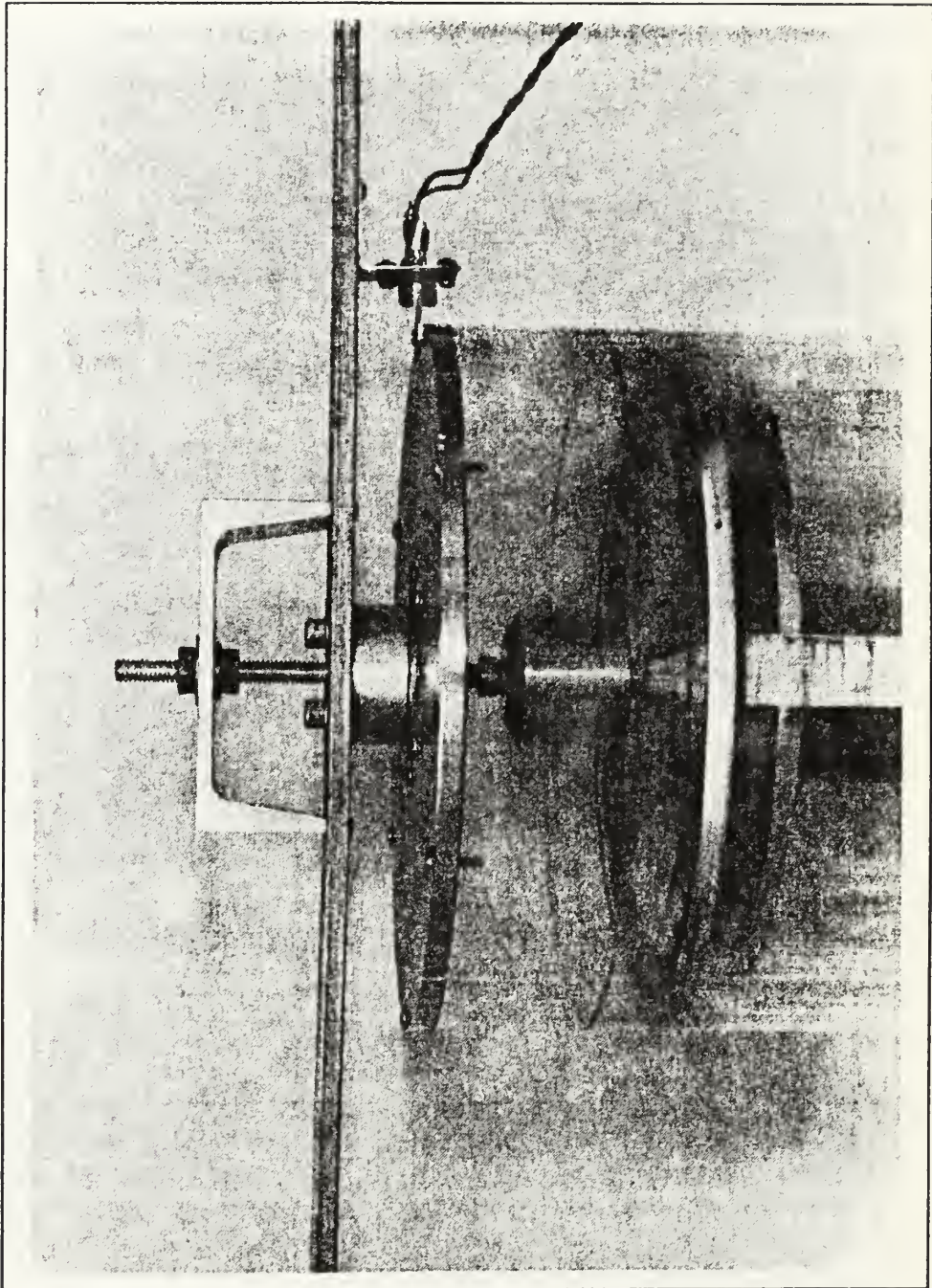
Figure 1 Taylor-Couette cell flow apparatus

Figure 2 Expanded view of the drive assembly

Figure 3 Expanded view of upper mounting

18

B. ELECTRICAL DESIGN

1. Transduction

Several constraints, mechanical as well as theoretical, led us to choose a piezoelectric polymer film as the source of cavity excitation. The polymer is polyvinylidene fluoride (PVDF). PVDF is sold commercially in sheet form, resembling a piece of thick plastic wrap. For our application, a 40μm thick strip was cut 2.0 cm wide and 50.8 cm long to match the length of the cavity. For a constant driving voltage, PVDF acts as a constant displacement source.

Our ultimate goal is to investigate changes in azimuthal mode structure due to the rotating flow. Consequently, it is not necessary to excite radial and vertical modes in order to observe the frequency split or shift. Choice of excitation frequency and source placement can limit excitation of these modes.

Since the PVDF strip is a constant displacement source, its width has to be less than one-half wavelength for the range of frequencies of interest. The upper frequency limit for preliminary testing was chosen to be 8kHz. Similar reasoning as that used for strip width was also applied to strip placement. With the strip extending across the length of the cavity, those vertical modes requiring a node at the mid-height of the cavity would be weakly excited, if at all.

19

2. Receiver

A 6.02 mm diameter electret microphone is embedded in the wall of the inner cylinder so that its face is flush with the surface of the cylinder. A silicone gel is placed around the microphone to provide a tight seal. The desire to minimize the number of penetrations through the cylinders during preliminary testing led us to use only one microphone placed at the vertical center of the cavity, 25.4 cm from either vertical boundary. However, the use of only one microphone and its placement necessarily limits the interpretation of the results of the preliminary testing as will be discussed in Chapter IV.

3. Angular Speed

The design uses a photo-interrupter to measure the angular speed of the outer cylinder. A small tab, mounted at the top of the outer cylinder, gates the output of the photo-interrupter once each revolution. The interrupter signal output is fed to an HP 5384A frequency counter which counts the number of events occurring within a .1, 1, or 10 second window. Digital readout could either be in hertz or the average period of revolution.

IV.   RESULTS OF PRELIMINARY TESTS

To assess the capabilities and limitations of our initial design, we performed two preliminary tests. The purpose of these tests was to verify our theoretical analysis of the cell and to determine the magnitude of errors caused by nonuniformities.

With the inner and outer cylinders fixed, the output of an HP 3562A dynamic signal analyzer was used to excite the cavity. A 5 Vrms periodic chirp source output, a fast sine sweep over the selected frequency span that repeats with the same period as the time record, was used. The output of the embedded electret microphone was fed back to the signal analyzer and its power spectrum obtained.

Frequencies corresponding to clearly discernable peaks in the power spectrum were recorded. The power spectrum was analyzed from d.c. to approximately 3.6 kHz in 400 Hz windows, having 0.5 Hz resolution. Within this frequency span, approximately sixty theoretical eigenfrequencies are possible. To aid in the resonant frequency cataloguing, an HP 3314A function generator was used in conjunction with the dynamic signal generator to manually sweep through a resonance and observe the phase change on an oscilloscope.

The results of these measurements are shown in Figure 4, which is a graph of observed resonance frequencies versus the

corresponding theoretical frequencies. The solid line has a slope of one. Ideally, the data points should fall on this line. The degree to which they do not is shown in Figure 6, which shows the magnitude of percent error. Generally, the results are quite good. The agreement is typically within 1%.

A number of modes were easily observable indicating the gap between the boundary rings and the cylinder walls did not kill the mode structure. The mode structures of interest, those with purely azimuthal dependence, were often masked by much stronger, closely spaced vertical modes. Vertical mode structures were not eliminated to the degree we had anticipated. This maybe due in part to the way the PVDF is attached. The strip is actually composed of two shorter strips, joined at the midpoint of the cavity. The joint construction may result in a smaller displacement of the PVDF at the joint as compared to the rest of the strip, therefore, allowing vertical modes to be excited. Further work in this area is needed.

The use of one microphone, located at the center of the cavity, is not sufficient to distiguish between closely spaced modes. A moveable probe microphone might be better suited for determining mode structure.

Lastly, we did not observe any purely azimuthal modes and only about half of the modes represented in Figure 4 have any azimuthal component. This again points to the need for continued work on the method of transduction.
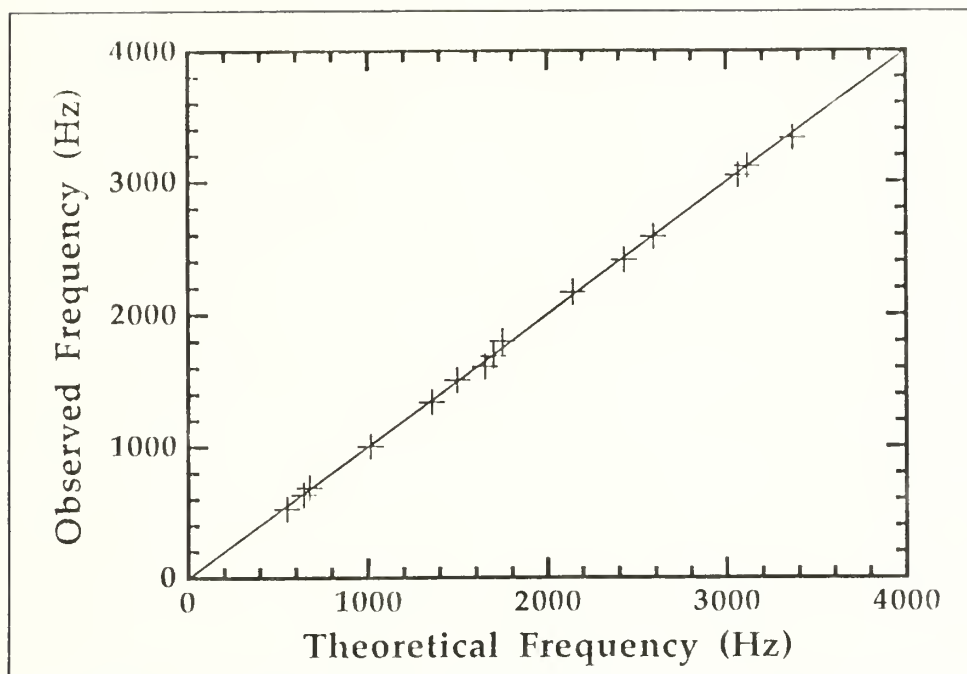
Figure 4 Observable resonance peaks from dc to 3.6kHz
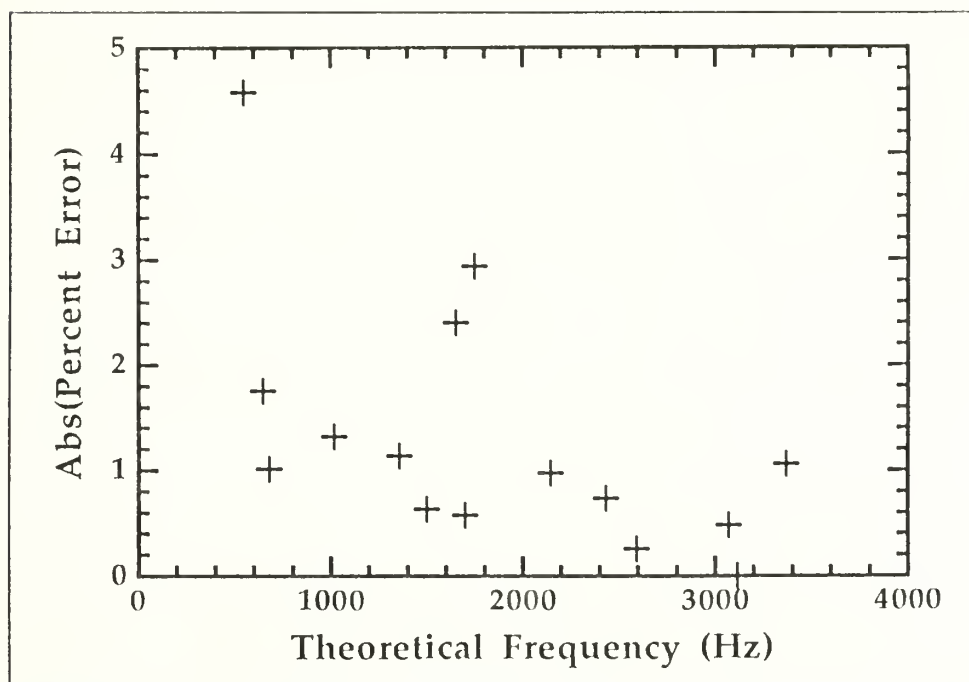
Figure 5 Agreement between observed resonance and theoretical resonance

While making the measurements discussed above, we noticed that the resonance frequency of a mode depended on the relative angular orientation of the inner and outer cylinders. We suspect that this is due to nonuniformities in the cylinder walls, ring boundaries, and alignment. The magnitude of this effect is illustrated in Figure 6. The data show the result of measurements of the resonance frequency at six equally spaced relative orientations. In Figure 6, the percentage variation of the resonance frequencies is plotted as a function of the mean resonance frequency. In all cases, the percentage variation is less than approximately 1.5%. This could account for much of the error shown in Figure 5.
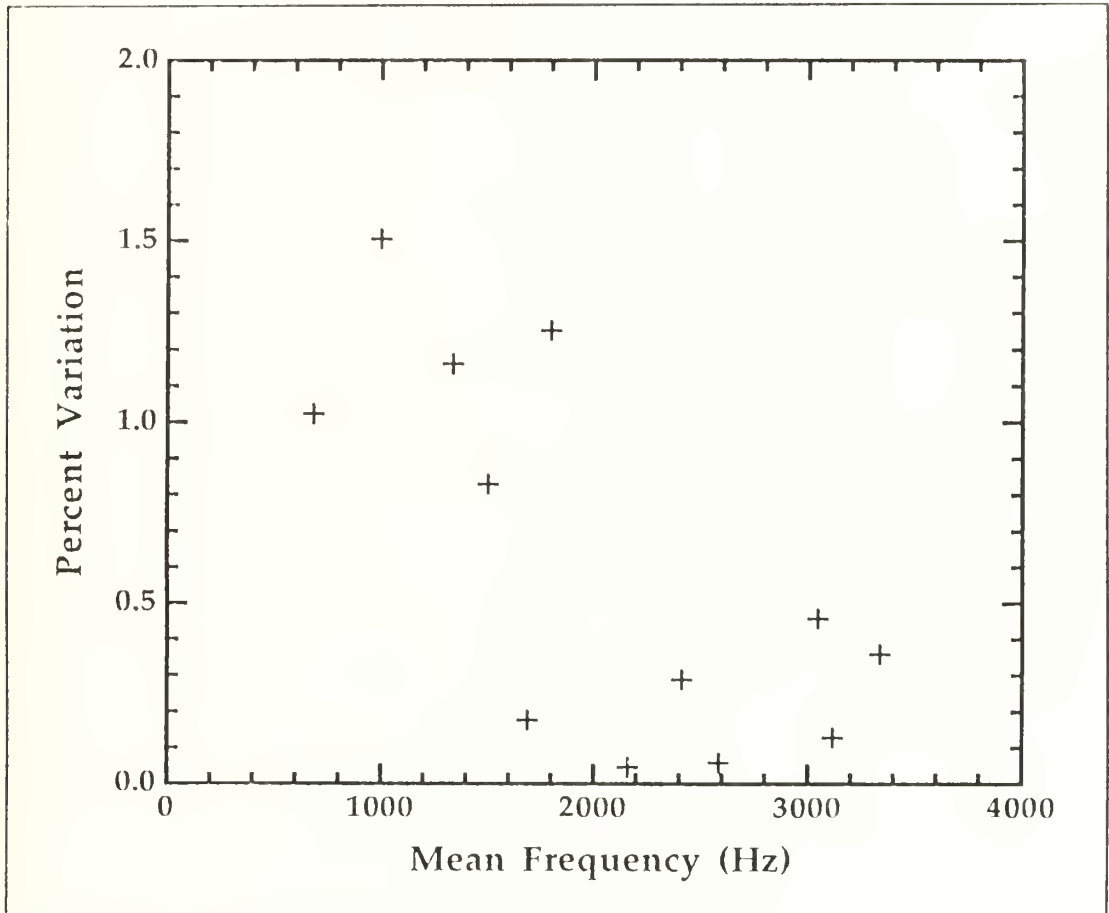
Figure 6 Variation of resonance through 360 degrees of rotation

V.   SUMMARY AND CONCLUSIONS

This thesis reports the design and construction of a Taylor-Couette cell. The apparatus uses acoustic transduction as a means to characterize global properties of the flow. Preliminary tests show that the static mode structure differs slightly from theoretical predictions, mainly because nonuniformities in the cavity. The nonuniformities were qualitatively observed by measuring the resonant frequencies for different angular positions of the transducer. These preliminary tests provide qualitative limitations imposed by the apparatus for the applicability of the theory in Chapter II. Because of nonuniformities, certain degeneracies are asymmetrically removed, mocking the effect of an arbitrary flow. Thus, quantitative knowledge of the effect due to nonuniformities is essential in order to determine the minimum differential rotation for which the effects due to the flow become important.

The acoustic "visualization" reported in this thesis constitutes a novel concept, but further development of the technique is required. As opposed to standard visualization methods, in principle acoustic transduction does not limit the Reynold's numbers for which the technique is useful. But most important, because the acoustic phase can provide global properties of an arbitrary flow, the investigations proposed

in this thesis may lay the foundations for a first-principles phenomenological theory of turbulence that relies on a complete set of global variables for its description.

APPENDIX

$$j_{mn}$$

m, n	j_{mn}
0, 0	0.0
1, 0	0.9487
2, 0	1.8975
3, 0	2.846
3, 0	3.795
5, 0	4.743
6, 0	5.692
7, 0	6.641
θ, 0	7.589
0, 1	28.8
●, 1	28.8
2, 1	28.8
3, 1	28.0
0, 2	57.6
1, 2	57.6

MODES OF A CYLINDRICAL ANNULUS

m,n\ l	0	●	2	4	4	5	6
0,0	0	339	678	1016	1355	1694	2033
1,0	549	645	872	1155	1462	1781	2106
2,0	1098	1149	1290	1496	1744	2019	2310
4,0	1646	1681	1780	1935	2132	2362	2616
4,0	2195	2221	2298	2419	2580	2773	2992
5,0	2744	2765	2826	2926	3060	3224	3415
4,0	3293	3310	3362	3446	3561	3703	3870
7,0	3842	3857	3901	3974	4074	4199	4346
4,0	4390	4403	4442	4506	4593	4706	4839
3,1	16661	16664	16674	16692	16716	16746	16784
1,1	16661	16664	16674	16692	16716	16746	16784
2,1	16716	16722	16732	16749	16773	16804	16842
3,1	16776	16780					
0,2	33321	33323	33328				
1,2	33321	33323	33328				

Cavity Height	Inner Radius	Outer Radius	R_o/R_i
50.838 cm	9.477 cm	10.510 cm	1.109

LIST OF REFERENCES

Andereck, C. David, Dickman, R., and Swinney, Harry L., "New Flows in a Circular Couette System with Co-Rotating Cylinders," Physics of Fluids, Vol. 26, p. 1395, June 1983.

Berry, M. V., Chambers, R. G., Large, M. D., Upstill, C., and Walmsley, J. C., "Wavefront Dislocations in the Aharonov-Bohm Effect and its Water Wave Analogue," European Journal of Physics, Vol. 1, pp. 154-162, 1980.

DiPrima, and Swinney, Harry L., Hydrodynamic Instabilities and the Transition to Turbulence, ed. by H. L. Swinney and J. P. Gollub, pp. 139-180, Springer-Verlag, 1981.

Donnelly, R. J., "Taylor-Couette Flow: The Early Day," Physics Today, Vol. 44, p. 32, 1991.

Larraza, A., unpublished work at the Naval Postgraduate School, 1989.

INITIAL DISTRIBUTION LIST

1. Defense Technical Information Center   2
    Cameron Station
    Alexandria, VA 22304-6145

2. Library, Code 052   2
    Naval Postgraduate School
    Monterey, CA 93943-5002

3. Andrés Larraza   2
    Physics Department, PH-Le
    Naval Postgraduate School
    Monterey, CA 93943-5002

4. Professor Anthony Atchley   2
    Physics Department, PH-Ay
    Naval Postgraduate School
    Monterey, CA 93943-5002

5. Bruce Denardo   2
    Physics Department, PH-De
    Naval Postgraduate School
    Monterey, CA 93943-5002

6. Lieutenant Kevin Blum, USN   1
    Naval Submarine School
    Code 80
    Groton, CT 06349-5700

7. Professor Karlheinz Woehler, Chairman PH   1
    Physics Department
    Naval Postgraduate School
    Monterey, CA 93943-5002

8. Professor Steven Garrett   1
    Physics Department, PH-Gx
    Naval Postgraduate School
    Monterey, CA 93943-5002